

Photocatalytic degradation of some endocrine disrupting compounds by modified TiO₂ under UV or halogen lamp illumination

Radina Kralchevska · Maria Milanova ·
Mirjana Bistan · Albin Pintar · Dimitar Todorovsky

Received: 14 December 2012 / Accepted: 29 March 2013 / Published online: 12 April 2013
© Akadémiai Kiadó, Budapest, Hungary 2013

Abstract For the first time, data on the effect of TiO₂ modification by N-doping or by carbon nanotubes on the photocatalytic destruction of endocrine disrupting compounds 17 α -ethynylestradiol (EE2) and 17 β -estradiol (E2) in aqueous solutions are reported. A possibility to accomplish photocatalytic process under halogen lamp irradiation is shown. The catalyst is prepared by a sol–gel method. During the synthesis process, it is modified by N-doping (1.8 % nitrogen) or by carbon nanotube addition (5 % of the TiO₂ mass). X-ray diffractometry, SEM, TEM, N₂ adsorption–desorption, X-ray photoelectron and UV–Vis diffuse reflectance spectroscopy are applied for characterization. The crystal structure, phase composition, crystallites size, specific surface area, pores average diameter, pore area and volume distribution, morphology, UV–Vis and X-ray photoelectron spectra of the materials are reported and discussed. An HPLC technique is used for estrogen analysis. The sorption ability and photocatalytic activity (measured by degradation rate constant and percentage of the pollutant conversion) of the catalysts under UV (150 W, emission maximum at 365 nm) or 150 W halogen lamp illumination are determined. Full destruction of E2 and >99.7 % of EE2 is reached after 2 h irradiation with halogen lamp.

Keywords Carbon nanotubes · Estrogens · N-doping · Photocatalysis · TiO₂

R. Kralchevska · M. Milanova · D. Todorovsky (✉)
Faculty of Chemistry and Pharmacy, University of Sofia, 1, J. Bourchier Blvd., 1164 Sofia, Bulgaria
e-mail: nhdt@wmail.chem.uni-sofia.bg

M. Bistan · A. Pintar
Laboratory for Environmental Sciences and Engineering, National Institute of Chemistry,
Hajdrihova 19, 1001 Ljubljana, Slovenia

Introduction

The steroids of concern for the aquatic environment due to their endocrine disruption potential are mainly estrogens and contraceptives, which include (E2) and 17 α -ethynylestradiol (EE2) [1]. Steroid drugs are frequently used in livestock to control the oestrous cycle, treat reproductive disorders and induce abortion [2]. This could greatly increase the generation of hormone steroids in urine [1]. The literature data on estrogens aqueous solubility vary in wide range but the values (mg/l) 1.51 ± 0.04 for E2 and 9.20 ± 0.09 for EE2 at pH 7, 25.0 ± 0.5 °C in Milli-Q reagent grade water [3] can be accepted as representative. Due to their solubility, both natural and synthetic estrogens enter the aquatic environment via wastewater treatment plant effluents or untreated discharges. Hence, these compounds can reach concentrations (normally in the ng/l range) that can be sufficient to exert estrogenic responses.

EE2 and bisphenol A (BPA) are the most frequently studied in environmental research due to their wide usage, low removal [4, 5] and high toxicity. EE2 is 10–50-fold higher than that of estrone (E1) and E2 [6]. Thus, the reduction/elimination of EE2 could have the biggest single impact on the estrogenicity of the effluent [7]. The median concentration (ng/l) of EE2 in sewage effluents in Germany, England, The Netherlands and the U.S. is 1/3 [8], in ground, raw and purified drinking water in Germany—up to 2.4 [8, 9]. However, *in vitro* studies have shown that exposure of wild fish to only 0.1 ng/l of EE2 may provoke feminization in some species of male [8, 10]. Occasionally, surprisingly high concentrations of EE2 have been reported—up to 273 ng/l in some U.S. streams and even 2 ng/l in drinking water [11, 12]. However, EE2 common concentrations in effluents are rather close to the present detection limits of most analytical techniques [7]. That is why one can suppose that although EE2 was not always detected, it may still be present in some effluents. Concentrations of E2 up to 20 ng/l were reported in effluents from wastewater treatment plants [13]. The estrogenic steroids have the ability to be adsorbed on aquatic sediments [14], thus they can act as environmental reservoirs and could become bioavailable [15].

Most important processes that play a role in the removal of estrogens are: adsorption, aerobic or anaerobic degradation, anoxic biodegradation and photolytic degradation. EE2 shows far most persistence [16]. Current wastewater treatment plants are normally designed for carbon, nitrogen and phosphorus removal, but a partial endocrine disruption compounds (EDCs) removal is often achieved simultaneously [17]. Special attention is paid on advanced processes, which allow high removal of recalcitrant compounds; however, many by-products are released that could have an estrogenic activity higher than their precursors [17]. Satisfactory results are reported using: granular activated carbon [18], fullerenes and small diameters single-wall carbon nanotubes [5], molecularly imprinted polymers [19]. More than 99 % degradation of EE2 in Lake Zurich water is achieved [20] by ozonation with slow reappearance of 0.1–0.2 % of the initial concentration [21]. Enzymatic (laccase-catalyzed) waste treatment [22] and fungal treatment (97 % removal of E2 and EE2 in 24 h) [23] also show successful results. The photolytic transformation of E2 and EE2 occurs with a quite low quantum yield [24], higher

pH values benefited the process [25]. The destruction of E2 proceeds under short wave UV irradiation (30 W, $\lambda_{\text{max}} = 253.7$ nm) but no effect is observed at treatment at $\lambda_{\text{max}} = 365$ nm (125 W) [26]. UV/H₂O₂ treatment is more effective but requires extended times [27].

Photocatalytic degradation of E2 on immobilized TiO₂ was first reported by Coleman et al. [28]. Photocatalysis coupled with photolysis is much more effective than photolysis alone [29–32]. One of the main advantages of TiO₂ is its potential to render complete mineralization [33]. The estrogenic activity of E2 is lost in the first step of the photocatalytic reactions under 365 nm-UV light [34].

Different types of photocatalytic reactors [28, 29, 31, 32, 35–37], substrates for TiO₂ immobilization (titanium alloys [28, 29, 32], polytetrafluoroethylene [32, 36], glass beads [38]) were tested. UV sources emitting different wavelength illumination (UVA [30, 31], UVC [31, 37]) and different power (150 W xenon lamp [28, 32, 37], 125 W Philips high-pressure mercury lamp [29], 15 W [35, 37]), placed at different distances from the treated solution have been applied. The influence of different TiO₂ concentration was also explored [39]. The presence of urea had negligible effect on the oxidation of EE2 and moderate one on E2 destruction [40].

The reported efficiency of E2 degradation vary from 50 % for 40 min to 98 % for 3.5 h [34, 39], 90 % for 20 min [32], 97 % for 4 h or 98 % for 1 h depending of the type of illumination [37]. Under UVA irradiation, in slurry with Degussa P25 TiO₂, the degradation of E1, E2 and EE2 in multicomponent EDCs mixture reaches respectively 49, 20 and 25 % after 180 min of irradiation. Under UVC, the conversions of E2, EE2 after 180 min are 60 % [31]. The first order rate decomposition constant (min^{-1}) varies depending of treatment conditions: 0.033, 0.050 [32], 0.106 [29], 0.15 [35] for E2 and 0.086 for EE2 [29].

Investigations on EDCs destruction mediated with more complicated TiO₂-based catalysts are rather limited. The doping of TiO₂ with 2 mol % Ag or Pt has no effect on the photocatalytic degradation or mineralization of all the EDCs at concentrations found in water [35].

All of the above considered studies are performed with TiO₂ Degussa P25 as photocatalyst under UV irradiation. To the best of our knowledge, neither N-doped TiO₂ or microcomposites TiO₂-nanotubes nor white or sun light have been used up to now to promote the degradation of estrogens in waste waters. At the same time, the advantage to carry out the process under visible/sun light illumination is obvious (suitable for combining with biological treatment for some estrogen conjugates [38], environmentally friendly).

The aim of the present paper is to investigate the possibilities of photocatalytic estrogen degradation under the action of UVA and halogen lamp illumination in the presence of sol-gel prepared TiO₂ modified by nitrogen doping or by addition of carbon nanotubes. Such materials have not been used for treating the estrogens containing waste waters yet. The structure, phase composition, morphology and some spectral properties of the prepared catalysts were studied and their sorption ability and photocatalytic activity on the E2 and EE2 degradation were determined. Commercially available Degussa TiO₂ P25 was used as referent material.

Experimental

Materials

Commercially available Degussa TiO₂ P25 (Degussa-Hüls AG, mentioned in the text as P25), Ti[OC₄H₉]₄ (Fluka, purum, >97 %), C₂H₅OH (p.a., 99.8 %), multi-walled carbon nanotubes MWNT-L-P (10–30 nm, purity 80 %, Sunny Co. Ltd., China, further labeled as NT), methanol (for HPLC, purity 99.9 %, Sigma-Aldrich) were used as starting materials. As model pollutants, estrogenic compounds EE2 and E2 (Sigma-Aldrich, 98 %, HPLC grade) were applied. NTs were preliminary treated in boiling in conc. HNO₃ [41] to decrease the content of Fe (the main impurity) and amorphous carbon as well as to activate their surface as a result of partial oxidation stimulating TiO₂-NT composite formation.

Synthesis of catalysts

TiO₂-N was synthesized by a controlled hydrolysis of ethanol solution of Ti[OC₄H₉]₄ by 25 % aqueous ammonia at room temperature [42]. After 60 min agitation, the suspension was dried (80 °C, 15 h) and calcined (350 °C, 1 h). The nitrogen content in the so prepared samples was 1.8–2 %, similar to the one applied by Xu et al. [43]. In the present work, material with 1.8 % nitrogen was used.

The TiO₂-NT was obtained following the method of Wang et al. [44]. Ethanol-water solution was added to ethanol-butoxide mixture, leading to the hydrolysis of the later. Just after the beginning of the hydrolysis, NTs (5 % of the mass of expected TiO₂) were added at vigorous stirring. After the aging of the sol (24 h), the gel was grinded, heated at 400 °C for 3 h and cooled to room temperature in N₂ flow to avoid NT oxidation. The temperature of heating and the gas flow ensure separation of eventually rested traces of organics. The content of NTs was chosen following findings of Yu et al. [45] for the best results reached in other photocatalytic systems. The conditions of the composite preparation ensure no appreciable degradation of the NTs during the synthetic process. Indeed, the determined (by the high-temperature ignition of the samples) carbon content in the final product agrees (within the limits of ±0.4 %) with the calculated value from initial ratio.

Catalysts characterization

The nitrogen content in the prepared sample was determined by the elemental analyzer Vario EL III V5.018. X-ray diffractograms were taken by Siemens D-500 powder diffractometer (Cu K_α, 40 kV, 30 mA) equipped with secondary monochromator to exclude K_β light. Quantitative analysis of diffractograms was performed by the Rietveld method using the program BRASS [46]. The film morphology of the same samples was observed by scanning (JEOL JSM 35CF) and transmission (JEOL HRTEM JEM 2100, 200 kV) electron microscopy. The surface area and porosity were measured by N₂ adsorption-desorption by means of Micromeritics ASAP 2020 MP/C instrument. Before measurements, the samples

(approx. 0.3 g) were degassed at 200 °C. Specimens' UV–Vis diffuse reflectance spectra were registered by Lambda 40P spectrophotometer (Perkin Elmer) equipped with a Praying Mantis accessory. X-ray photoelectron spectroscopy was done in UHV chamber of ESCALAB-MkII (VG Scientific) at 10^{-5} Pa. The C2s of CH₂ at 285 eV was used for spectra calibration.

Photocatalytic tests

Stock solutions of E2 and EE2 (3 g/l) were prepared in methanol and stored in a freezer (−20 °C) as recommended in [14]. Shortly before the experiments, working solutions with concentration of 0.3 mg/l (or 1.101 μM for E2 and 1.012 μM for EE2) containing 0.01 % methanol (such an ethanol concentration is used by Coleman et al. [29]) were prepared using ultrapure water (18.2 MΩ cm). These estrogenic working solutions were used for the photocatalytic tests in a batch slurry reactor. The working solutions as well as aliquots withdrawn during the oxidation were stored for not more than 24 h in a refrigerator.

The photocatalytic activities of catalysts were tested under the following conditions: volume of reaction suspension 250 cm³, catalyst concentration 0.5 g/l, magnetic stirring speed 600 rpm, and air flow rate 330 ml/min. The reached agitation of the slurry excludes the influence of transport phenomena on the adsorption and photodegradation reactions kinetics. After a 30 min “dark” period (for the establishing of equilibrium of the sorption process), the system was illuminated by a UV high-pressure mercury 150 W lamp (emission in the 300–400 nm region with a maximum at ~360 nm) or 150 W halogen lamp. The lamps were laid in a Pyrex tap water cooling jacket, immersed perpendicularly in the suspension. The double-walled constructed reactor ensures constant cooling of the investigated suspension by outer water flow (~5 °C) using a thermostat (Julabo, model F25). The temperature of the suspension was always maintained at 20 ± 1 °C. The aliquots from the solution (subjected to irradiation for a certain period of time) were filtered through Whatman filter (0.45 μm pores) and subjected to subsequent analysis.

From the relation $\ln(C/C_0)/t$ (C_0 —the initial concentration after the dark period, C —the concentration after t min irradiation), accepting first order kinetics, the apparent reaction rate constants of the degradation process were determined, excluding the effect of the pollutant sorption on the catalyst. The sorption ability of the latter was determined from the relation $(C_{00} - C_0)/C_{00}$ (C_{00} —the initial estrogens concentration before the dark period).

Analytical procedure

A solid phase extraction as a preconcentration method for water sample analysis was based on previous reports [14, 47, 48]. Oasis HLB extraction cartridge type 6 cc-500 mg with a polymeric water-wettable reversed-phase sorbent, particle size 60 μm, pore size 80 Å, pH range 0–14 was chosen for the procedure. The cartridges were conditioned consequently with 4 ml of methanol and 4 ml of ultrapure water prior to use. The 250 ml samples were allowed to pass through the cartridges under vacuum. Then the cartridge was rinsed with 4 ml of 5 % aqueous-methanol solution

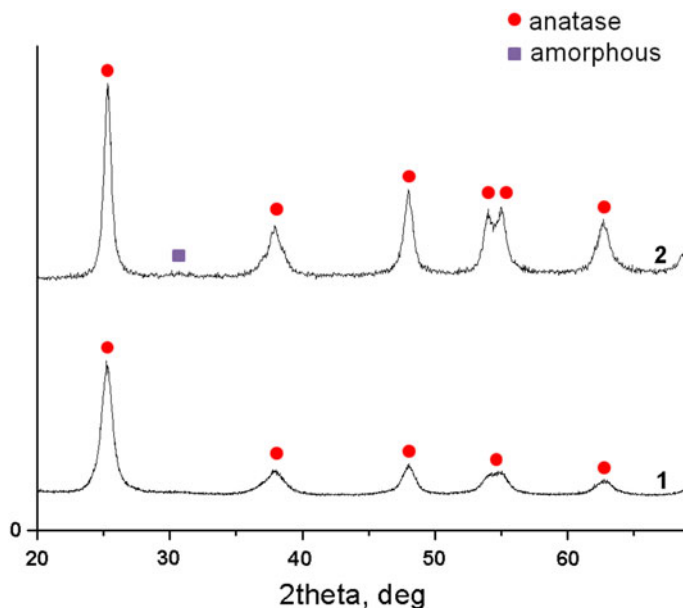


Fig. 1 X-ray diffractogram of TiO₂ prepared at 350 °C (1) and N-doped TiO₂ (2)

and dried under a nitrogen flow. The evaluation of the compound of interest was done with 4 ml of methanol. The samples were dried under nitrogen stream up to the volume of 1 ml. Each sample was analyzed twice by means of isocratic HPLC technique and average values were further considered.

The instantaneous concentration of the pollutant was determined by using an HPLC instrument (Hewlett Packard, model 1100) equipped with Phenomenex Luna C18 column (25 cm × 4.6 mm, 5 μm) under the following conditions: mobile phase water/methanol (volumetric ratio 25/75), flow rate 0.8 cm³/min, column temperature 30 °C, injection volume 20 μl, UV 210 nm detection. Calibration curves for both pollutants are linearly best fitted ($R^2 = 0.9992$ for EE2 and 0.9854 for E2). The uncertainty of HPLC analysis was characterized by the relative standard deviation of the signal (0.04 %), calculated from three parallel analyses of a sample containing 0.3 mg/l EE2.

Results and discussion

Catalysts physicochemical characterization

Crystal structure and phase composition

The X-ray diffractograms (XRD) of pure and N-doped TiO₂ prepared at 350 °C TiO₂ are shown in Fig. 1. The conditions of catalyst synthesis result in the formation of anatase only. The lattice parameters of the samples are listed in Table 1 along with

Table 1 Lattice parameters, size of crystallites and content of anatase in the studied samples

Sample	Parameters	Value
JCPDS 73-1764	a, b (Å)	3.77600
	c (Å)	9.48600
	V (10 ⁶ pm ³)	135.25
Degussa TiO ₂ P25	a, b (Å)	3.785(4)
	c (Å)	9.505(3)
	V (10 ⁶ pm ³)	136.20
	Crystallite size (nm)	16.1
	Anatase content (%)	82
TiO ₂ , produced at 350 °C	a, b (Å)	3.782(7)
	c (Å)	9.472(2)
	V (10 ⁶ pm ³)	135.53
	Crystallite size (nm)	9.4
	Anatase content (%)	100
N-doped TiO ₂	a, b (Å)	3.792(2)
	c (Å)	9.501(6)
	V (10 ⁶ pm ³)	136.60
	Crystallite size (nm)	12.3
	Anatase content (%)	100

data for Degussa P25. The parameters of the N-doped product are slightly enlarged compared with the pure sample prepared at the same temperature of annealing. This increase can be explained with interstitial positions of the nitrogen.

The crystallite size (Table 1) of the product prepared at 350 °C is considerably smaller than that of the commercial product. The difference is due to difference in the heating temperature in the course of catalyst synthesis. The role of this factor is confirmed by the fact that, working in the same temperature interval, similar in size crystallites (7.5 nm) are obtained independently of the synthesis method applied [49, 50]. The N₂ doping leads to small increase of the size, related to the increase of cell parameters and reaching values similar to these reported by Shao et al. [51].

Morphology

Fig. 2 shows SEM images of the prepared catalysts. The sol–gel synthesized TiO₂ has a globular structure with grains considerably larger than those of the commercial product, 200–500 nm in size for the material obtained at 350 °C, inclined to agglomeration. The grains of the N-doped catalyst are much smaller with irregular form and a high degree of agglomeration. TiO₂ crystallites, approx. 10 × 10 nm and smaller, are seen on the TEM image of the composite TiO₂-NT (Fig. 3).

Specific surface area and porosity

Fig. 4 shows nitrogen adsorption–desorption isotherms of the examined samples. The isotherm of the commercial product is rather similar to the one observed by Yu

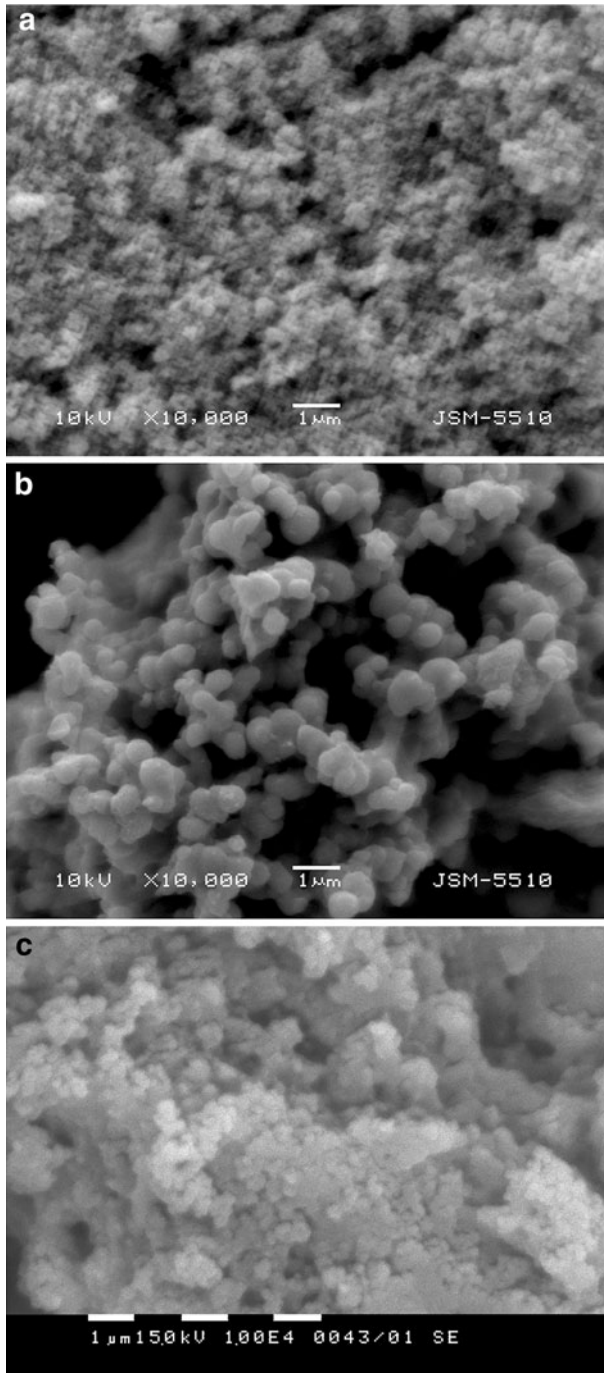
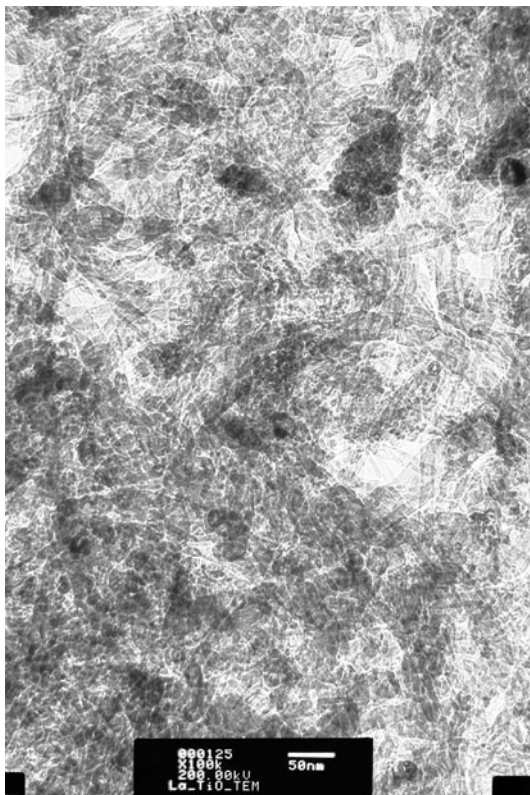


Fig. 2 SEM images of Degussa TiO₂ P25 (a), sol-gel synthesized TiO₂ heated at 350 °C (b) and of the N-doped catalysts (c); scale bar 1 μm

Fig. 3 TEM image of sol-gel prepared TiO_2 with 5 % NTs



et al. [52] and can be described as type IV. The H3 type hysteresis loop (appeared at $p/p_0 = 0.85$ – 1.0) suggests the presence of slit-like pores usually resulted from the particle aggregation. The sharp drop of N_2 adsorbed amount in desorption curve indicates mesoporosity of the product.

The modified sol-gel prepared products show the same type of isotherm. The observed large H2 type of hysteresis with an inflection of nitrogen adsorbed volume at $p/p_0 = 0.45$ is indicative for well-developed mesoporosity and existence of pore cavities larger than the openings.

The calculation of pore size distribution (Fig. 5) was performed by analyzing the adsorption data of the N_2 isotherm using the Barrett–Joyner–Halenda (BJH) method with Halsey–Kruk–Jaroniec–Sayari correction implemented in the software provided with the ASAP 2020 adsorption apparatus. In the latter procedure, the Kelvin equation in the form $r[\text{nm}] = -0.953/\ln(p/p_0)$ was used and the statistical film thickness was represented by the Halsey equation $t[\text{nm}] = 0.354[-5/\ln(p/p_0)]^{0.333}$.

As far as the pollutant molecule diameter is $\sim 15 \text{ \AA}$, pores above this width are namely of interest. Results for specific area and pores diameter, volume and area are summarized in Table 2. Our previous study [53] shows a significant influence of the synthetic method on the textural properties of the N-doped TiO_2 . The doping by the

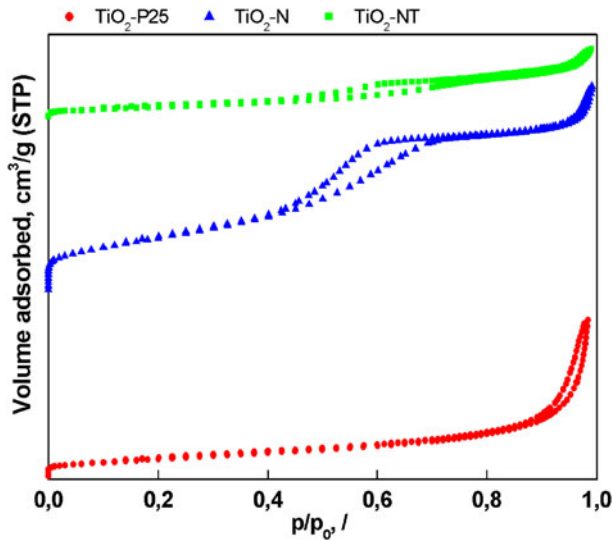


Fig. 4 N_2 adsorption–desorption isotherms of Degussa TiO_2 P25, TiO_2 -N and TiO_2 -NT

method chosen in the present paper practically does not change the properties of the undoped product prepared at the same temperature [54]. The BET surface area of the doped product is similar to that obtained by Shao et al. [51], but the average pore diameter is more than an order higher than in the latter material. The difference has to be ascribed to the difference in the method of catalyst preparation, N-source used and content of the dopant in the final product.

The pore area the TiO_2 -NT composite shows (Fig. 5c) monomodal distribution around pores with an average diameter of about 7 nm. The pores volume distribution seems more likely to bimodal one (Fig. 5a).

UV-Vis spectra

The UV-Vis diffuse reflectance spectra of synthesized materials are shown in Fig. 6. It can be seen that the commercial product Degussa TiO_2 P25 exhibits some absorption in the visible part of the spectrum. It is known that due to presence of Ti^{3+} , TiO_2 powders show absorption in the wavelength region longer than 400 nm. Ti^{3+} can be formed as a result of TiO_2 reduction at elevated temperatures [55, 56]. Accounting for the Degussa TiO_2 P25 production mode [44, 56], such reduction seems possible. However, our EPR study does not confirm presence of measurable amount of Ti^{3+} and the P25 visible light absorption has to be ascribed to charge transfer with the rutile nanoparticles that have a smaller band gap of 3.0 eV as suggested by Hurum et al. [57].

The N-doped product shows two absorption edges (the second one expressed as a shoulder) and increased visible light absorption in the region 400–550 nm. The result can be assigned to the substitution of O in crystal lattice with N species. This statement is in agreement with the ab initio calculations showing that the optical

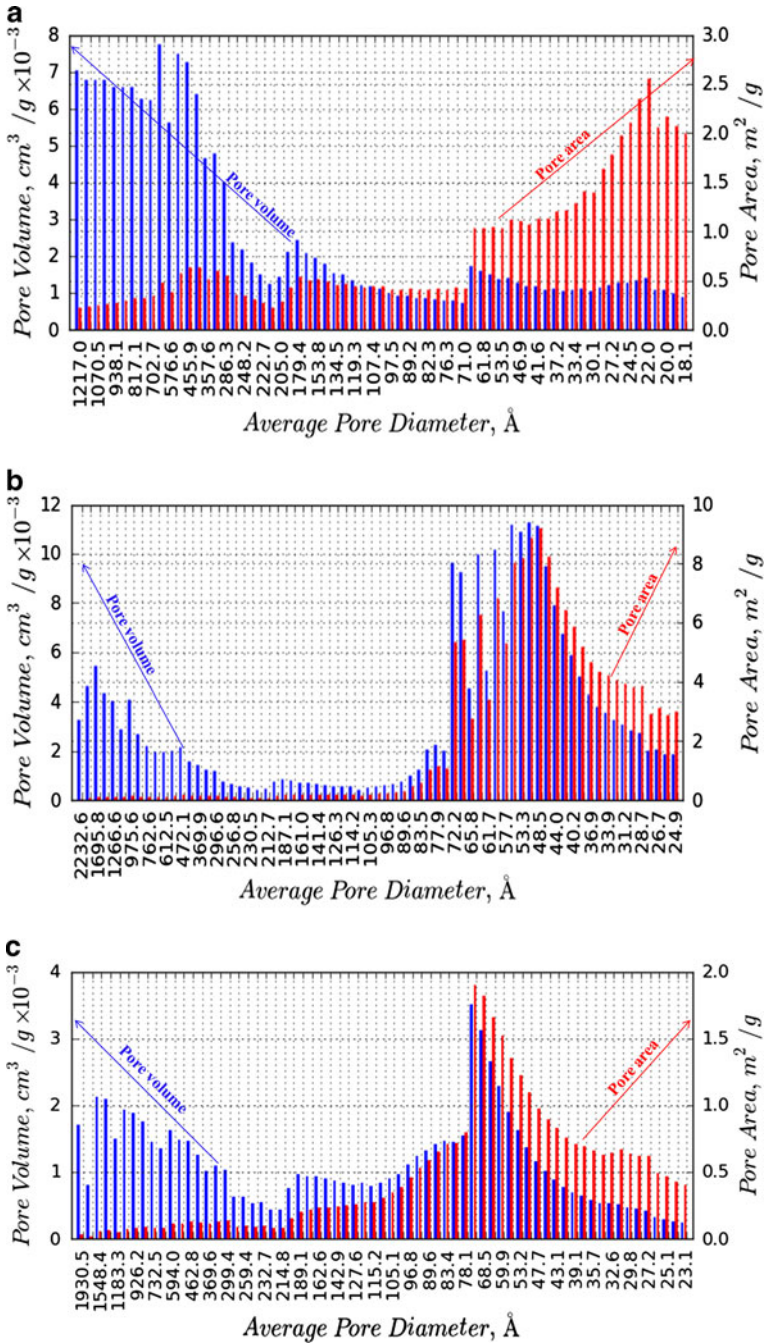
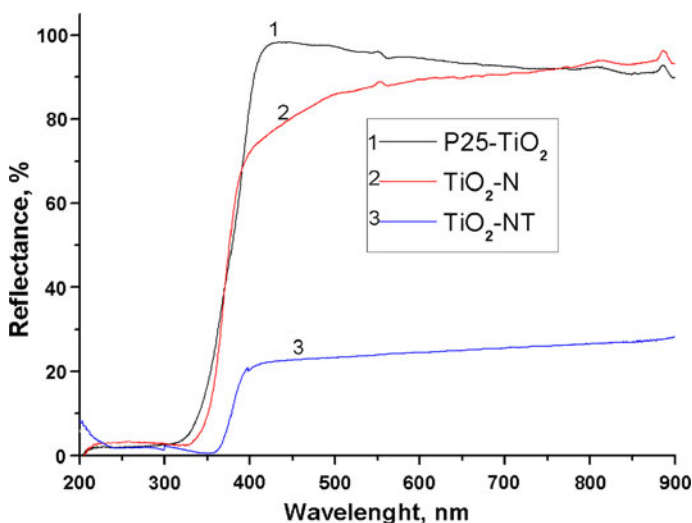


Fig. 5 Pore volume and surface area distribution as a function of pore diameter for Degussa TiO₂ P25 (a), N-doped catalysts (b) and TiO₂-NT composite (c)

Table 2 Textural properties of the synthesized catalysts

Parameter	Degussa TiO ₂ P25	TiO ₂ -N, 350 °C	TiO ₂ -NT, 400 °C
BET surface area (m ² /g)	52.0	141.5	34.4
Total pore volume (cm ³ /g)	0.17	0.22	0.08
Average pore diameter (BJH) (Å)	125.4	59.4	88.7
Micropore volume, × 10 ⁻⁵ , cm ³ /g	3.1	- ^a	9.8
Micropore area (m ² /g)	1.89	- ^a	1.29

^a Micropores (<4.6 Å) are not registered in the sample

**Fig. 6** UV-Vis diffuse reflectance spectra of examined catalyst samples

absorption of nitrogen-doped TiO₂ in the visible light region is primarily located between 400 and 500 nm [58].

The low reflectance of the TiO₂-NT composite is due to its black color.

X-ray photoelectron spectra

The X-ray photoelectron spectra (XPS) of TiO₂-N reveals peaks (eV) of O1s (530.15), Ti2p_{3/2} (459.0), Ti2p_{1/2} (464.7), N1s (401.1), C1s (285.0). The traces of carbon most probably originate from the measuring equipment.

The location of the N1s peak observed in the present paper (401.1 eV) suggests the presence of interstitial nitrogen (the peak at 400 eV is accepted as an indication of nitrogen in such position in [58], also). The peak is asymmetric. A low intensity component at 396.0 eV was observed, which is due to Ti-N bonds formed when the N atoms replaced the oxygen in the TiO₂ crystal lattice. The latter result is in agreement with the above mentioned result from UV-Vis spectroscopy.

Catalysts sorption ability

Data listed in Table 3 show that the sorption ability depends on the nature of the pollutant as well as on the applied catalyst, and these two factors are interconnected. Specific surface area is an important but not a crucial factor determining the catalyst sorption performance. Indeed: (i) The sorption of E2 is $\sim 10\%$ stronger than that of EE2 on Degussa P25 or $\text{TiO}_2\text{-NT}$ and 2.5-times higher on $\text{TiO}_2\text{-N}$. (ii) The sorption capacity of the N-doped catalyst is two-fold lower (experiments 5, 6, Table 3) or slightly higher (exp. 11, 12) than that for Degussa TiO_2 P25 despite the almost three-fold larger surface area of the former (Table 2). (iii) The composite $\text{TiO}_2\text{-NT}$ exhibits 3–6-fold higher sorption ability than TiO_2 P25 and $\text{TiO}_2\text{-N}$ (exp. 2, 3, 5; 8, 9, 11) despite its smaller surface area (Table 2). However, the sorption of the herbicide iodosulfuron on Degussa TiO_2 P25, pure and N-doped TiO_2 follow other dependence on the specific surface area but again without simple proportionality between the two parameters [54].

The reported facts show that no simple relation “specific surface area–sorption ability” exists in the studied systems. It has to be concluded that chemical peculiarities of the catalyst surface and its interaction with the pollutant are of primary importance for the sorption processes. This conclusion is in agreement with the results reported in [5] showing that although the availability of surface sorption sites controls adsorption, the later is related to molecular conformation of EDCs, also.

Photocatalytic degradation

Data for reaction rate constant and the degree of estrogens degradation are summarized in Table 3 and partially illustrated in Fig. 7. In some cases, the results for TiO_2 P25 reveal two-stage processes with very different rate constants. In this connection, the calculated average constants can be considered as a strongly tentative evaluation, only (Table 3).

The preliminary experiments show much better performance of the modified catalysts than the pure TiO_2 , sol–gel prepared material after heating at $350\text{ }^\circ\text{C}$. The degradation rate constants obtained with unmodified TiO_2 are approximately half- (UV irradiation) or one (halogen lamp illumination) order lower. That is why the further experiments were done with the modified catalysts and Degussa TiO_2 P25 was used as referent material.

Catalysts behavior at UV illumination

Considering the average value of reaction rate constants for P25, NT doped titania shows faster degradation of EE2 than TiO_2 P25 (exp. 2, 3, Table 3). More importantly, $\text{TiO}_2\text{-NT}$ degrades the pollutant completely in 60 min. In contrast, a momentary photocatalytic activity of P25 is observed up to 15 min illumination followed by a much slower degradation process and P25 continues to maintain low but stable hormone concentrations. A similar inhibition of TiO_2 P25 after 20 min irradiation is reported at other photocatalytic systems [59, 60].

Table 3 Sorption ability and apparent degradation rate constants obtained during the photolytic/photocatalytic oxidation of model pollutants over various catalysts

No.	Pollutant	Catalyst	Illumination	Sorption (%)	Rate constant, n (10^{-3} min^{-1})	Correlation coefficient	Reminder (%) after irradiation	
							60 min	120 min
1	EE2	Photolysis	UV	–	26.8 ± 0.1	0.9671	20.3	
2		TiO ₂ -NT		80.7	102.6 ± 0.4	0.9461	0	
3		TiO ₂ P25		26.8	346.1 ± 0.1^a	0.9999	0.30	
					10.5 ± 5.0^b	0.8974		
					Average: 77.8 ± 2.0	0.5715		
4		Photolysis	Halogen lamp	–	1.4 ± 0.04	0.8059	83.0	
5		TiO ₂ -N		13.4	50.6 ± 0.2	0.9924	0.22	
6		TiO ₂ P25		26.8	176.9 ± 0.1^a	0.9999	0.22	
					9.5 ± 4.9^b	0.9081		
					Average: 42.2 ± 2.0	0.5912		
7	E2	Photolysis	UV	–	21.1 ± 0.2	0.8748	26.8	
8		TiO ₂ -NT		91.2	94.2 ± 0.5	0.9035	0	
9		TiO ₂ P25		29.0	398.7 ± 0.1	0.9999	0	
10		Photolysis	Halogen lamp	–	1.8 ± 0.1	0.7771	83.3	82.0
11		TiO ₂ -N		33.0	66.9 ± 0.1	0.9972	1.8	0
12		TiO ₂ P25		29.0	196.8 ± 0.1^a	0.9999	0.27	0.25
					1.2 ± 0.1^b	0.4815		
					Average: 40.2 ± 2.3			

^a First stage of the process^b Second stage of the process

The TiO₂-NT catalyst managed to degrade completely E2 in 60 min (exp. 8, Table 3) but slower than TiO₂ P25; the latter giving the same effect for 30 min (exp. 9).

The NTs alone exhibit no measurable catalytic effect on the pollutant degradation—under conditions identical to the ones used in the above described experiments, the apparent degradation rate constant in the presence of only NTs is practically the same (within the error limits) as the one found at photolysis. Few factors can be responsible for the synergistic effect on the activity of the composite catalysts: (i) despite the difference in the methods used, it is clear from Figs. 3 and 4 that the grain size of TiO₂ in the composite with NTs is smaller than that without NTs. (ii) Despite that the surface area of the composite remains significantly smaller than that of pure TiO₂ or P25, the sorption ability of the former is much higher (Table 3). This is an indication for predominant selective adsorption of the pollutant on the surface of NTs. It is seen (Fig. 4) that the grains of TiO₂ are partly coated on the NTs. If one assumes a stronger sorption of the estrogen on the free surface of NTs, it will bring it in a close contact with the TiO₂. (iii) More probable mechanism

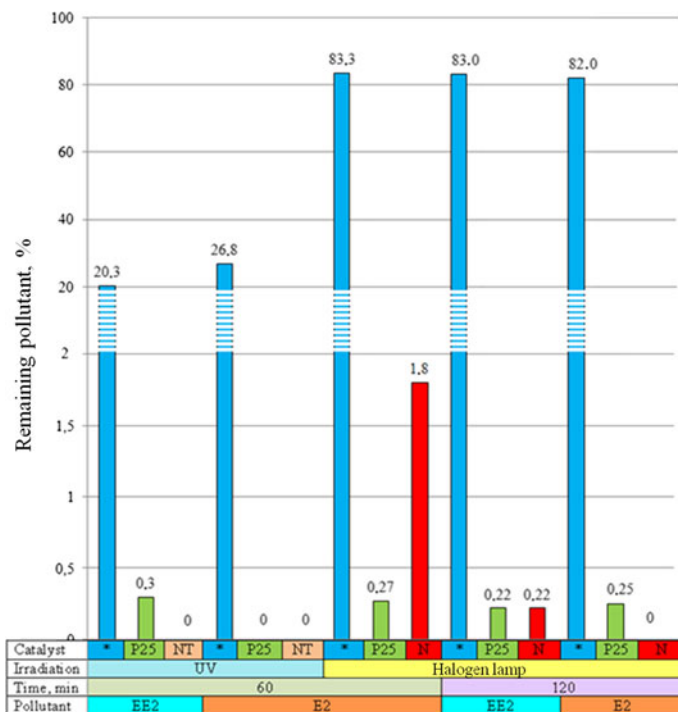


Fig. 7 Remaining pollutants (%) after illumination with UV-light with $\lambda_{max} = 365$ nm and with halogen lamp in the presence of different catalysts; *, no catalyst, i.e. photolysis only

of the synergistic effect is the action of NTs as a photosensitizer [61, 62]. The above mentioned close contact between TiO_2 and NTs as well the small grain size of TiO_2 in the composite ensure possibility the excited electrons in conduction band of TiO_2 to move towards NTs. The later process decreases the possibility of recombination of the e^-/h^+ pairs. O_2 adsorbed on the surface of NTs may accept e^- and form O_2^- , one of the main oxidizing agent in the system.

Catalysts behavior at halogen lamp illumination

Combining the XRD, XPS and UV–Vis results it must be concluded that in the N-doped catalyst nitrogen takes both interstitial and substituting positions in the TiO_2 lattice. The ionizations at both 396 and 400 eV may exert opposite effects decreasing the TiO_2 –N effectiveness. Nevertheless, at halogen lamp illumination, the latter catalyst ensures complete removal of E2 and >99.7 % of EE2 for 120 min (exp. 5, 11, Table 3). Although the concentration of the pollutant decreases rapidly in the beginning of reaction in presence of P25, a plateau occurred in the later stage in which the concentration of estrogens decreases negligibly as a function of time. So, a time period of 120 min was not sufficient for TiO_2 P25 to achieve complete removal of both compounds (runs 6, 12, Table 3). Domination of TiO_2 –N is also seen from the values of degradation rate constants (considering the TiO_2 P25 constant average value, Table 3).

Despite that, rather high efficiency of Degussa TiO₂ P25 under halogen lamp illumination (Table 3; Fig. 7) is not common and is hardly to be explained with a weak UV component in the spectrum of the illumination source used. It has to be supposed that the adsorbed pollutant plays some mediation role in the TiO₂ excitation. The mechanism proposed by Paul et al. [63] for the fluoroquinolone photocatalytic oxidation in presence of TiO₂ could be considered as a possible explanation of the obtained experimental results. The formation of a complex between the pollutant and the TiO₂ causes red shift in the pollutant absorption spectrum (due to charge transfer from the ligands to the metal under the visible light action) and electron transfer to the TiO₂ conduction band. Further on, the process proceeds following the commonly accepted mechanism. Generally speaking, the observed effect is in accordance with the conclusion made by Shao et al. [51] that the measured band-gap energy value can not be regarded as a direct response to the level of photocatalytic activity.

Estrogens inclination to degradation

Generally, the rate constants for both studied estrogens are similar which can be expected accounting for the similarity between the two chemical structures. E2 degradation is slightly faster in the presence of Degussa TiO₂ P25 (with ~ 10 % for both UV and halogen lamp illumination) and of TiO₂-N catalyst (with ~ 15 %) compared to EE2 removal. Complete destruction of E2 is achieved using P25, in contrast with EE2 removal. The NT-containing composite shows the opposite effect causing a slightly faster destruction of EE2.

Literature data on this issue are limited to the action of TiO₂ P25 only and contain some controversies. The results obtained in the present paper confirm the results reported in [29, 35] (UVA illumination) and differ from the findings [31] for slightly easier destruction of EE2 at UVA or UVC illumination. As a whole, these results suggest a cross connection between the estrogen chemical nature and variations in photocatalytic conditions (such as light intensity, oxygen/air aeration) on the destruction susceptibility of the estrogens.

Table 4 provides the possibility to compare the effectiveness of some methods for the photocatalytic degradation of E2 and EE2. It is seen that complete destruction of E2 and 99.7 % from the initial amount of EE2 (from 1.1 and 1 μM starting pollution solutions, respectively) can be reached even under halogen lamp irradiation applying the catalysts proposed in the present paper.

Conclusion

The paper gives description of crystal structure and textural properties of sol-gel prepared TiO₂, doped with nitrogen or carbon nanotubes, and their sorption and photocatalytic performance against some estrogenic compounds. The results concerning pure and doped TiO₂ are compared with those obtained with the commercial product Degussa P25. The synthetic method applied leads to both substitution of crystal lattice O to N species and the presence of interstitial nitrogen

Table 4 Effectiveness of some methods for photocatalytic degradation of E2 and EE2

Reference	Estrogen		Illumination	Rate constant, $k \times 10^{-3} \text{ min}^{-1}$	Degradation (%) for time (h)
	Type	Initial concentration (μM)			
[30]	E2	3	125 W, UVA, UVB, UVC	174	–
	EE2	3		231	–
[34]	E2	1	200 W, UVA		100–3
[31]	E2	1	UVA		20–3
	EE2		UVA		25–3
	E2,EE2		UVC		60–3
[28]	E2	0.05–3	150 W xenon lamp	15.7	50–0.7; 98–3.5
[32]	E2	0.33	15 W, UV, 0.24 mW/cm ²	33	98–1
[36]	E2	0.914	1.2 mW/cm ² , UV	150	
[29]	E2	0.036	UVA	106	
	EE2	0.033	UVA	86	
[37]	E2	0.002	150 W, 238–579 nm	14	97–4
	E2		15 W, UVC	42	98–1
This work	E2	1.1	150 W, UVA	399 ^a	100–1
	EE2	1.0		103 ^b	100–1
	E2	1.1	150 W, halogen lamp	67 ^c	100–2
	EE2	1.0		177/9.5 ^{a,d}	>99.7–2

Catalyst: ^a P25, ^b TiO₂-NT, ^c -TiO₂-N, ^d two-stage process

content. The chemical peculiarities of the catalyst surface and its interaction with the pollutant are of primary importance for the sorption processes.

For the first time, data on the effect of TiO₂ modification by N-doping or carbon nanotubes on photocatalytic destruction of E2 and EE2 as well as the possibility to achieve their removal under halogen lamp irradiation are reported.

The commercial product P25 showed significant degradation efficiency for both estrogens under UV irradiation. However, in some cases, its activity sharply declines after the first 15–30 min of illumination. That is why, as a final result, the catalysts TiO₂-NT and TiO₂-N show similar or better efficiency despite the fact that their main component (the pure sol–gel synthesized TiO₂) is much less effective than Degussa P25. The studied catalysts ensure full destruction of E2 and >99.7 % of EE2 after 2 h halogen lamp irradiation with rather low-intensity UV component.

Acknowledgments The work was performed under the financial support of the Bulgarian Fund for Scientific Investigations (Contract DO 02-93/08), Slovenian Research Agency (Research Program P2-0150), and NATO Science for Peace Program (Contract SFP 982835).

References

1. Ying G-G, Kookan RS, Ru Y-J (2002) *Environ Int* 28:545–555
2. Refsdal AO (2000) *Anim Reprod Sci* 60:109–119
3. Shareef A, Angove MJ, Wells JD, Johnson BB (2006) *J Chem Eng Data* 51:879–881
4. Braga O, Smythe GA, Schafer AI, Feitz A (2005) *J Environ Sci Technol* 39:3351–3358
5. Pan B, Lin D, Mashayekhi H, Xing B (2008) *Environ Sci Technol* 42:5480–5485
6. Segner H, Navas JM, Schafers C, Wenzel A (2003) *Ecotoxicol Environ Saf* 54:315–322
7. Johnson AC, Sumpter JP (2001) *Environ Sci Technol* 35:4697–4703
8. Heberer T (2002) *Toxicol Lett* 131:5–17
9. Adler P, Steger-Hartmann T, Kalbfus W (2001) *Acta Hydrochim Hydrobiol* 29:227–241
10. Purdom CE, Hardiman PA, Bye VJ, Eno NC, Tyler CR, Sumpter JP (1994) *Chem Ecol* 8:275–285
11. Johnson AC, Ternes T, Williams RJ, Sumpter JP (2008) *Environ Sci Technol* 42:5390–5399
12. Kolpin DW, Furlong ET, Meyer MT, Thurman EM, Zaugg SD, Barber LB, Buxton HT (2002) *Environ Sci Technol* 36:4007–4008
13. Desbrow C, Routledge EJ, Brighty GC, Sumpter JP, Waldock M (1998) *Environ Sci Technol* 32:1549–1558
14. Lei B, Huang S, Zhou Y, Wang D, Wang Z (2009) *Chemosphere* 76:36–42
15. Petrović M, Eljarrat E, López de Alda MJL, Barceló D (2001) *Trends Anal Chem* 20:637–648
16. de Mes T, Zeeman G, Lettinga G (2005) *Rev Environ Sci Biotechnol* 4:275–311
17. Auriol M, Filali-Meknassi Y, Tyagi RD, Adams CD, Surampalli RY (2006) *Process Biochem* 41:525–539
18. Snyder SA, Adham S, Redding AM, Cannon FS, DeCarolis J, Oppenheimer J, Wert EC, Yoon Y (2007) *Desalination* 202:156–181
19. Meng Z, Chen W, Mulchandani A (2005) *Environ Sci Technol* 39:8958–8962
20. Huber MM, Canonica S, Park G-Y, Gunten UV (2003) *Environ Sci Technol* 37:1016–1024
21. Huber MM, Ternes TA, Gunten UV (2004) *Environ Sci Technol* 38:5177–5188
22. Auriol M, Filali-Meknassi Y, Tyagi RD, Adams CD (2007) *Water Res* 41:3281–3288
23. Blánquez P, Guieysse B (2008) *J Hazard Mater* 150:459–462
24. Mazellier P, Méité L, Laat JD (2008) *Chemosphere* 73:1216–1223
25. Liu B, Wu F, Deng N-S (2003) *J Hazard Mater* 98:311–316
26. Liu B, Liu X (2004) *Sci Total Environ* 320:269–274
27. Rosenfeldt EJ, Linden KG (2004) *Environ Sci Technol* 38:5476–5483
28. Coleman HM, Eggins BR, Byrne JA, Palmer FL, King E (2000) *Appl Catal B* 24:L1–L5
29. Coleman HM, Routledge EJ, Sumpter JP, Eggins BR, Byrne JA (2004) *Water Res* 38:3233–3240
30. Coleman HM, Abdullh MI, Eggins BR, Palmer FL (2005) *Appl Catal B* 55:23–30
31. LiPuma G, Puddu V, Tsang HK, Gora A, Toepfer B (2010) *Appl Catal B* 99:388–398
32. Nakashima T, Ohko Y, Tryk DA, Fujishima A (2002) *J Photochem Photobiol A* 151:207–212
33. Gültekin I, Ince NH (2007) *J Environ Manage* 85:816–832
34. Ohko Y, Iuchi K, Niwa C, Tatsuma T, Nakashima T, Iguchi T, Kubota Y, Fujishima A (2002) *Environ Sci Technol* 36:4175–4181
35. Coleman HM, Chiang K, Amal R (2005) *Chem Eng J* 113:65–72
36. Nakashima T, Ohko Y, Kubota Y, Fujishima A (2003) *J Photochem Photobiol A* 160:115–120
37. Zhang Y, Zhou JL, Ning B (2007) *Water Res* 41:19–26
38. Mitamura K, Narukawa H, Mizuguchi T, Shimada K (2004) *Anal Sci* 20:3–4
39. Mai J, Sun W, Xiong L, Liu Y, Ni J (2008) *Chemosphere* 73:600–606
40. Karpova T, Preis S, Kallas J (2007) *J Hazard Mater* 146:465–471
41. Xia X-H, Jia Z-J, Yu Y, Liang Y, Wang Z, Ma L-L (2007) *Carbon* 45:717–721
42. Wang YQ, Yu XJ, Sun DZ (2007) *J Hazard Mater* 144:328–333
43. Xu J-H, Dai W-L, Li J, Cao Y, Li N, He H, Fan K (2008) *Catal Commun* 9:146–152
44. Wang W, Serp P, Kalck P, Silva CG, Faria JL (2008) *Mater Res Bull* 43:958–967
45. Yu Y, Yu JC, Yu J-G, Kwok Y-C, Che Y-K, Zhao J-C, Ding L, Ge W-K, Wong P-K (2005) *Appl Catal A* 289:186–196
46. Birkenstock J, Fischer RX, Messner T (2003) BRASS 1.0 beta: The Bremen Rietveld Analysis and Structure Suite. Zentrallabor für Kristallographie und Angewandte Materialwissenschaften, Fachbereich Geowissenschaften, University of Bremen, Bremen
47. Jeannot R, Sabik H, Sauvard E, Dagnac T, Dohrendorf K (2002) *J Chromatogr A* 974:143–159

48. Trenholm RA, Vanderford BJ, Holady JC, Rexing DJ, Snyder SA (2006) *Chemosphere* 65:1990–1998
49. Xie Y, Yuan C (2004) *Appl Surf Sci* 221:17–24
50. Bubacz K, Choina J, Dolat D, Borowiak-Paleń E, Moszyński D, Morawski AW (2010) *Mater Res Bull* 45:1085–1091
51. Shao G-S, Wang F-Y, Ren T-Z, Liu Y, Yuan Z-Y (2009) *Appl Catal B* 92:61–67
52. Yu J, Yu H, Cheng B, Zhou M, Zhao X (2006) *J Mol Catal A Chem* 253:112–118
53. Kralchevska R, Milanova M, Hristov D, Pintar A, Todorovsky D (2012) *Mater Res Bull* 47:2165–2177
54. Kralchevska R, Milanova M, Pintar A, Todorovsky D (2012) *Mater Chem Phys* 133:1116–1126
55. Ohno T, Sarukawa K, Tokieda K, Matsumura M (2001) *J Catal* 203:82–86
56. Bickley RI, Gonzalez-Carreno T, Lees JS, Palmisano L, Tilley RDJ (1991) *J Solid State Chem* 92:178–190
57. Hurum DC, Agrios AG, Crist SE, Gray KA, Rajh T, Thurnauer MC (2006) *J Electron Spectrosc Relat Phenom* 150:155–163
58. Dunnill CWH, Aiken ZA, Pratten J, Wilson M, Morgan DJ, Parkin IP (2009) *J Photochem Photobiol A* 207:244–253
59. Hori Y, Bandoh A, Nakatsu A (1990) *J Electrochem Soc* 137:1155–1161
60. Xu A-W, Gao Y, Liu H-Q (2002) *J Catal* 207:151–157
61. Tian W, Yang H, Fan X, Zhang X (2010) *Catal Commun* 11:1185–1188
62. Yu Y, Yu JC, Chan C-Y, Che Y-K, Zhao J-C, Ding L, Ge W-K, Wong P-K (2005) *Appl Catal B* 61:1–11
63. Paul T, Miller PL, Strathmann TJ (2007) *Environ Sci Technol* 41:4720–4727